

Supporting Information

Multistep synergistic modified NaNbO₃-based ceramics for high-performance electrostatic capacitors.

Ling Lv¹, Zhongbin Pan^{1*}, Jiawen Hu¹, Zhixin Zhou¹, Huanhuan Li¹, Xiqi Chen¹, Jinjun Liu^{1*}, Peng Li², and Jiwei Zhai^{3*}

¹School of Materials Science and Chemical Engineering, Ningbo University, Ningbo, Zhejiang, 315211, China. E-mail: panzhongbin@163.com, liujinjun1@nbu.edu.cn

²School of Materials Science and Engineering, Liaocheng University, Liaocheng, Shandong, 252059, China.

³School of Materials Science & Engineering, Tongji University, 4800 Caoan Road, Shanghai 201804, China. E-mail: apzhai@tongji.edu.cn

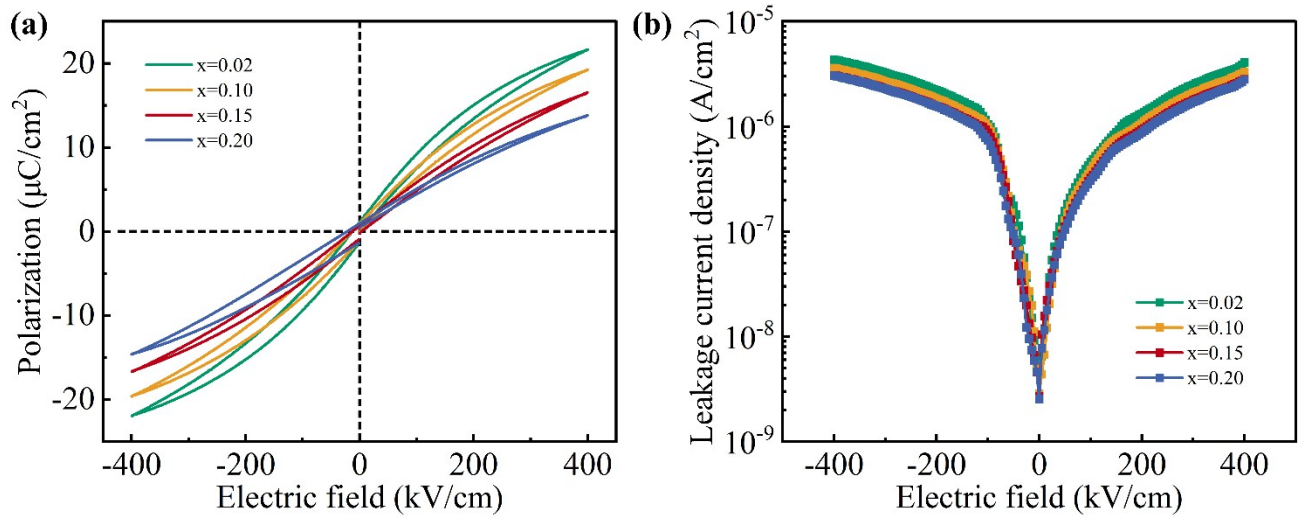


Figure S1. (a) Bipolar P-E loops of the NNCZ-xBH ceramic under 400 kV/cm electric field. (b) The leakage current density of NNCZ-xBH ceramics.

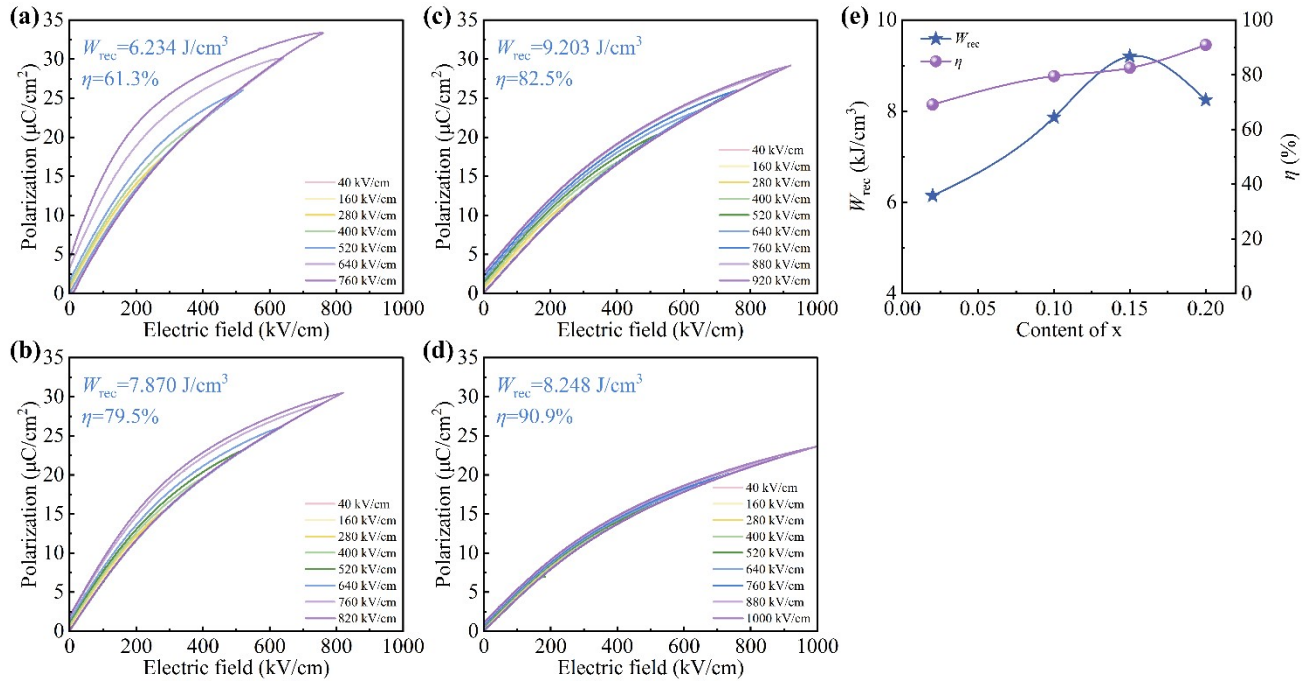


Figure S2. The unipolar P - E loops for NNCZ-xBH ceramics with the as electric field increases. (a) $x = 0.02$. (b) $x = 0.10$. (c) $x = 0.15$. (d) $x = 0.20$. (e) The calculated W_{rec} and η for NNCZ-xBH ceramics.

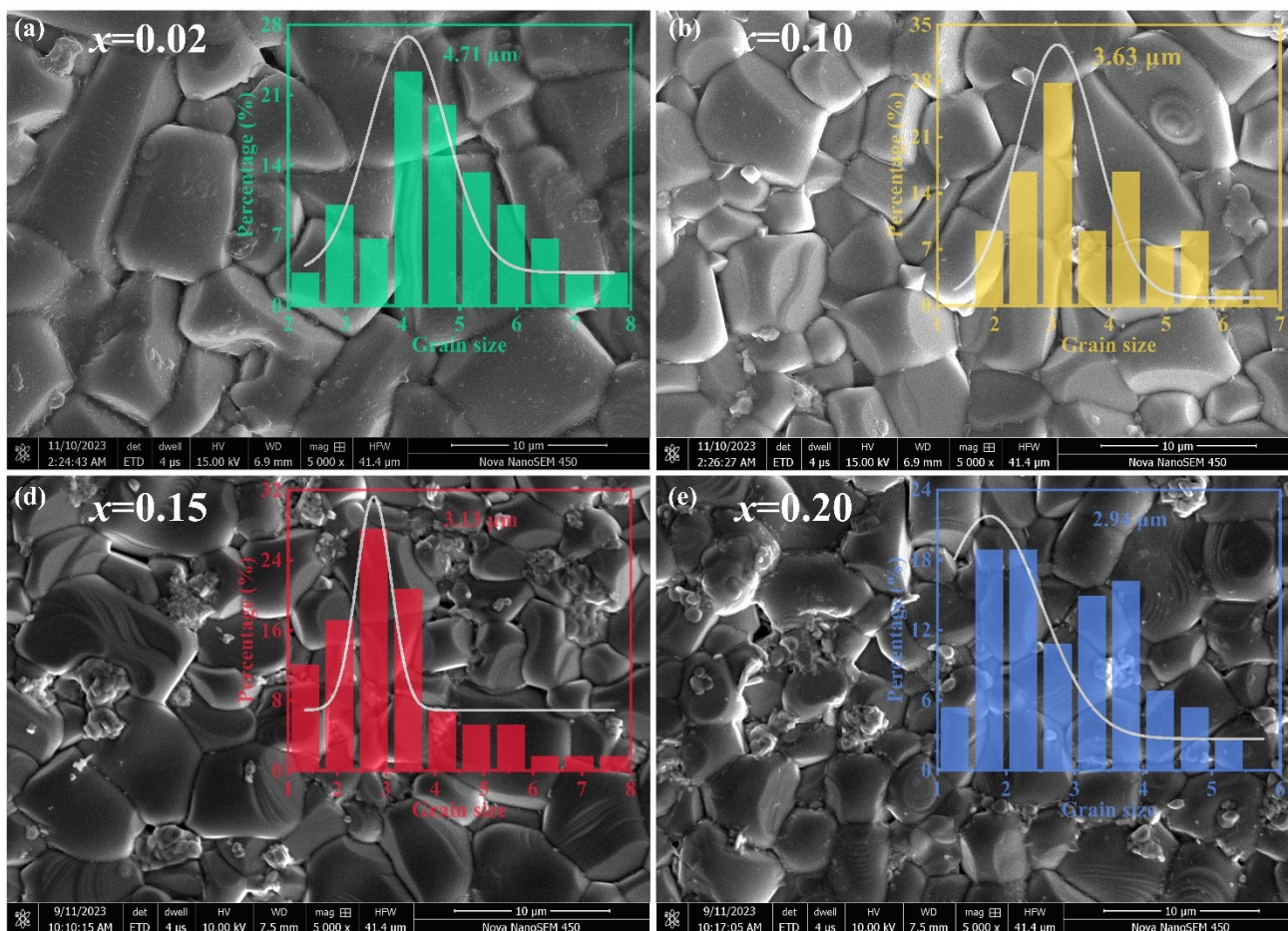


Figure S3. SEM micrographs on the thermally etched fractured surface of NNCZ-xBH ceramics. (a) $x = 0.02$. (b) $x = 0.10$. (c) $x = 0.15$. (d) $x = 0.20$. The inset of each figure corresponds to the statistical analysis of grain size distribution.

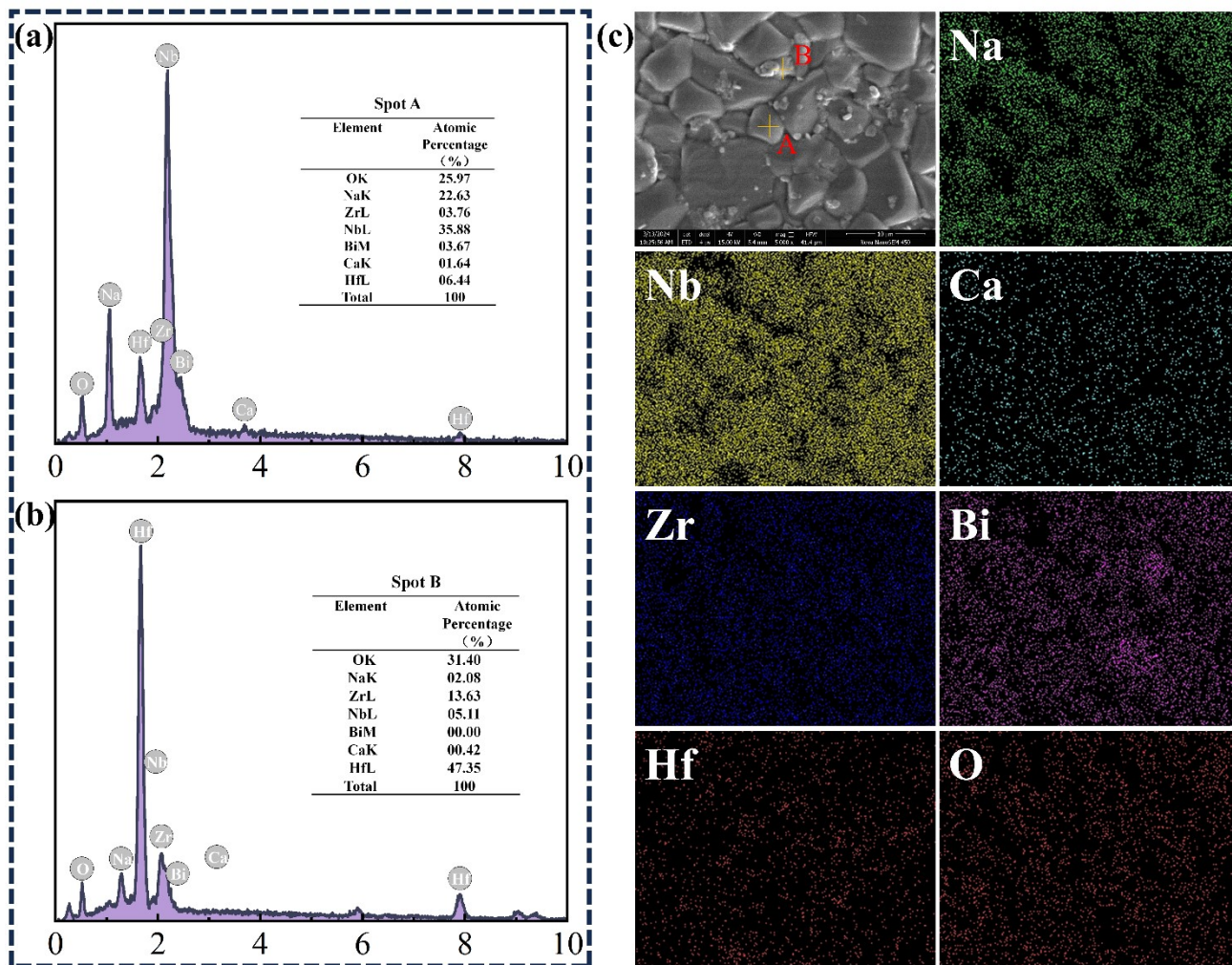


Figure S4. Energy spectrum and elemental distributions for the NNCZ–0.15BH ceramics.

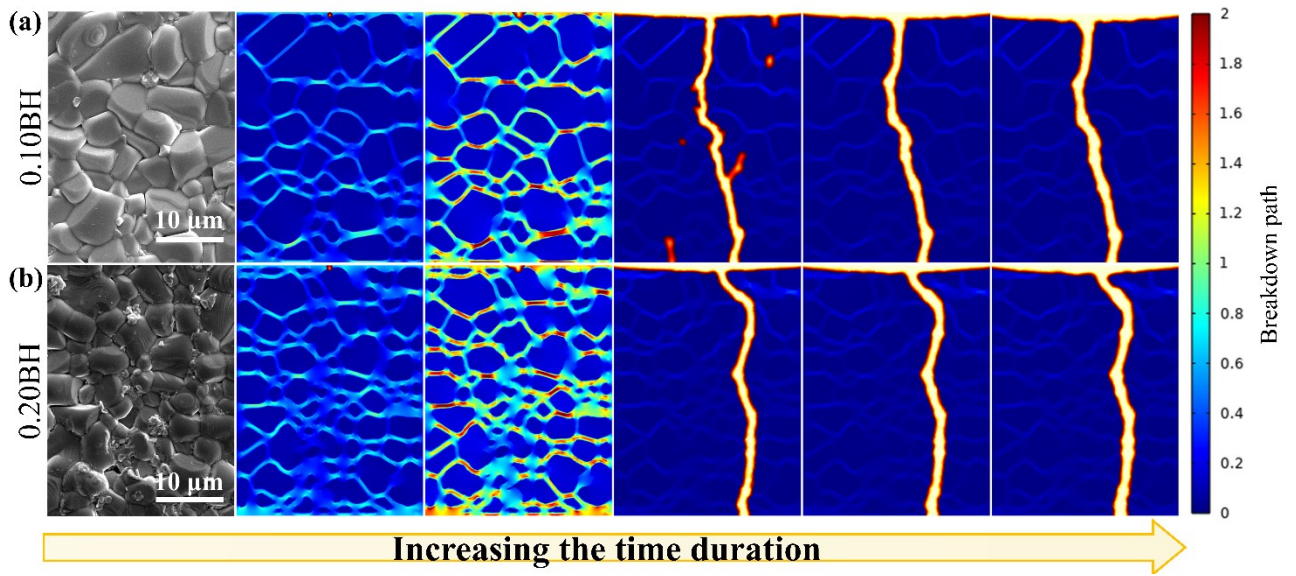


Figure S5. Phase field simulation of the breakdown path of (a) NNCZ-0.10BH ceramic and (b) NNCZ-0.20BH ceramic under the critical electric field.